Synthesis of Fe-doped Nickel oxide nanostructures via a simple mechanochemical route and its application for photocatalytic removing of MB

Rahmatollah Rahimi*, Mohammad Bozorgpour, Mahboubeh Rabbani

Department of Chemistry, Iran University of Science and Technology, Narmak, Tehran 16846-13114, Iran
E-mail: Rahimi_rah@iust.ac.ir

Abstract

Iron-doped nickel oxide ($Fe_{0.05}Ni_{0.99}O$) nanoparticles were prepared by ball milling the stoichiometric powder mixture of $NiCl_2.4H_2O$ and $FeCl_3.6H_2O$ and citric acid and calcined at 550 ^{0}C for 5 h. The phase composition and the structure of the calcined products were investigated by X-ray diffraction and scanning electron microscopy techniques, respectively. Then the potential of the obtained photocatalyst in degradation of methylene blue dye was studied under visible irradiation.

Key words: Fe-doped NiO, photocatalyst, Methylene blue

1. Introduction

Among transition metal monoxides, Nickel monoxide (NiO) is a highly interesting strongly correlated electron system [1-3]. Magnetism in NiO appears due to superexchange interaction between Ni ions. Different kinds of magnetic phase mainly depend on sign and the relative strength of the nearest neighbor and next nearest neighbor exchange interactions [4]. The doping of aliovalent metal ions into a NiO lattice modifies electronic and magnetic properties. Dilute magnetic systems have attracted much attention because of complex magnetic spin order [5]. Magnetic properties of randomly diluted NiO and CoO by divalent alkaline Mg have been studied in details [6,7]. Experimentally it was found that the crystal structure of both parent compounds does not change and also the lattice parameter does not change considerably upon dilution by Mg.

The antiferromagnetic ground state of NiO can be tuned by replacing Ni by other 3d transition metal ions. It has been found that Fe doped NiO nanoparticles reveal room temperature ferromagnetism.

In this work, Iron-doped nickel oxide ($Fe_{0.05}Ni_{0.99}O$) nanoparticles were prepared by ball milling the stoichiometric powder mixture of $NiCl_2.4H_2O$ and $FeCl_3.6H_2O$ and citric acid and calcined at 550 ^{0}C for 5 h. The phase composition and the structure of the calcined products were investigated by X-ray diffraction and scanning electron microscopy techniques, respectively. Then the potential of the obtained photocatalyst in degradation of methylene blue dye was studied under visible irradiation.

2. Experimental

2.1. Materials and Methods

All of the Chemicals used in this work were analytical grade reagents and used without further purification. Nickel nitrate ($Ni(NO_3)_2.6H_2O$), $Fe(NO_3)_2.9H_2O$ and citric acid were purchased from Merck company. Deionized water was used to prepare all solutions.

The samples were characterized by X-ray powder diffraction (XRD) using JEOL X-ray diffractometer with Cu Kα radiation. The particle morphologies of the NiO powder were observed by an AIS2100 (Seron Technology) scanning electron microscopy (SEM). The FT-IR analyses were carried out on a Shimadzu FTIR-8400S spectrophotometer using a KBr pellet for sample preparation. DRS spectra were prepared via a Shimadzu (MPC-2200) spectrophotometer.

2.2. Preparation of NiO nanoparticles

Fe doped NiO nanoparticles was synthesized by Using a ball-mill mechanochemical technique at 2000 rpm at room temperature for 20 min. $Ni(NO_3)_2$; $6H_2O$, $Fe(NO_3)_2.9H_2O$ and citric acid were employed as starting raw materials. The molar ratio of Fe:Ni was 5:95 and molar ratio of $Ni(NO_3)_2 \cdot 6H_2O$:citric acid was 1:3. The resultant was placed into a tube furnace, and calcined at 550 ◦C for 5 h in air.

2.3. Photocatalysis procedure

In a typical process, the catalytic reaction was carried out in a 100 ml photoreactor (Scheme 2), which contain 50 ml of MB dye (20 mg/l) solution and 0.05 g of catalyst. Before the irradiation, the solution was stirred in the dark (15 min) to allow equilibrium of the system. Irradiation was carried out using 400 W tungsten lamps as the light sources. All photocatalytic experiments were carried out at the same conditions. The distance between photoreactor and light sources was 20 cm. Samples (3 ml) were collected during the irradiation and MB solution were separated from the photocatalyst by centrifugation. The degradation was monitored by measuring the absorbance amount using a double beam UV–vis spectrophotometer (Shimadzu UV-1700) at 664 nm wavelength.

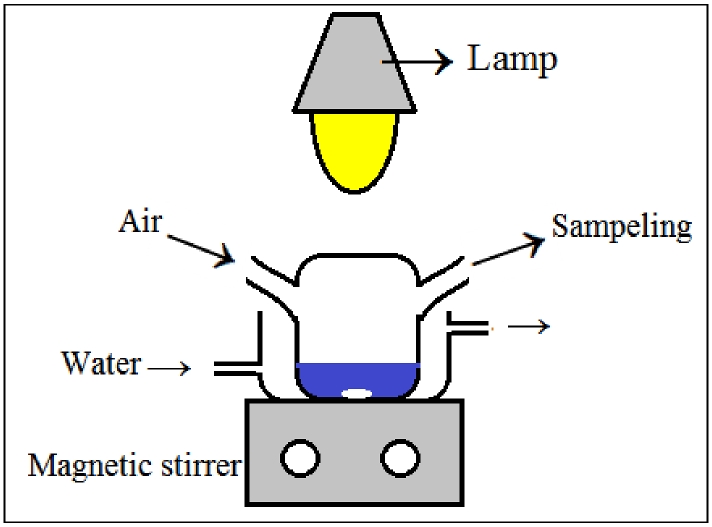

Scheme 1. Schematic representation of the photoreactor.

3. Results and discussion

3.1. Morphological characterizations

The morphology of the prepared Fe doped NiO nanoparticles was examined from SEM image, as shown in Fig. 1. It was found that all synthesized NiO nanoparticles were quite uniform in size.

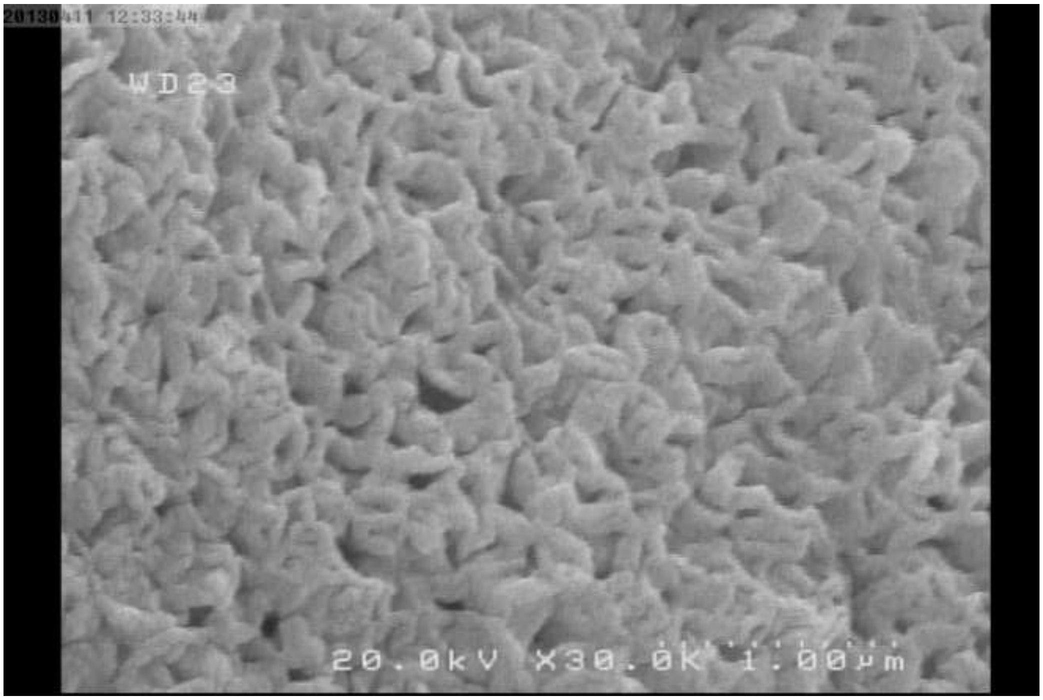

Fig. 1. The SEM images of the synthesized Fe doped NiO nanoparticles.

3.2. The X-ray powder diffraction

Fig. 2 shows the XRD pattern of Fe doped NiO nanoparticles. It can be seen that all these peaks are in good agreement with cubic NiO (JCPDS Card, No. 00-001-1239). No peaks, any else phase of NiO or impurity peaks are observed, which indicates the high purity of the obtained NiO nanoparticles and Fe ions doped at its phase. On the whole, these diffraction peaks suggesting that the sample is well crystallized.

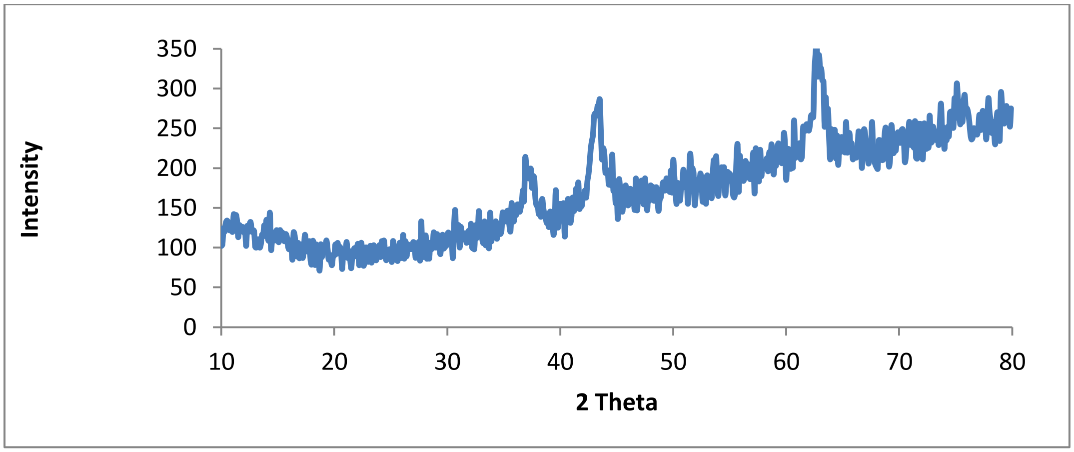

Fig. 2. The XRD pattern of the synthesized Fe doped NiO nanoparticles.

3.3. Optical properties

The UV–vis diffuse reflectance spectra (DRS) of the synthesized Fe doped NiO nanoparticles is shown in Fig. 3.

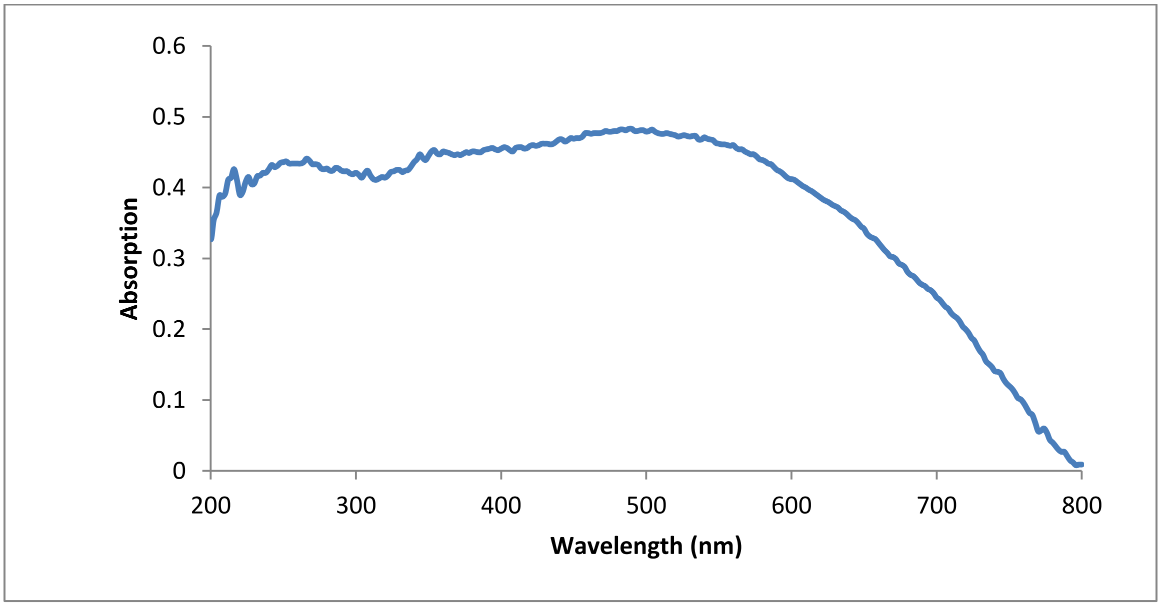

Fig. 3. The diffuse reflectance spectra (DRS) of the synthesized Fe doped NiO nanoparticles.

3.4. Fourier transforms infrared spectroscopy

Fig. 4 shows the FT-IR spectra of the Fe doped NiO nanoparticles measured in the range of 390–4000 cm^{-1}. The appearance of a sharp band at 450 cm^{-1} in the FT-IR spectra confirms the synthesis of NiO because it is the characteristic absorption band for the Ni–O stretching vibration. Additionally broad absorption peaks centered at around 3300-3500 cm^{-1} is caused by the O–H stretching of the absorbed water molecules because the nanocrystalline materials exhibit a high surface to volume ratio.

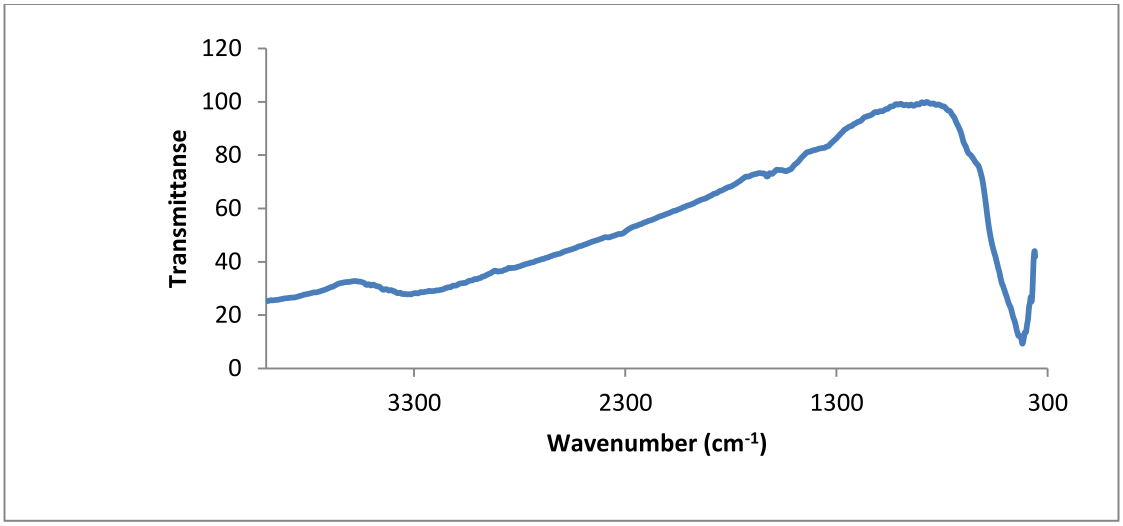

Fig. 4. The FT-IR spectrum of the synthesized Fe doped NiO nanoparticles.

3.5. Photocatalytic degradation of methylene blue

The photocatalytic activities of as-synthesized two kinds of catalysts were evaluated by the degradation of organic dyes methylene blue in aqueous solution under light irradiation. The Fe doped NiO nanoparticles, with a high specific surface area, were used as photocatalysts for the decomposition of methylene blue by the superoxides and/or hydroxyl radicals formed at their interface. The characteristic absorption of MB at 664 nm was chosen to monitor the photocatalytic degradation process. Concerning the initial MB concentration, it can be concluded that there was a decrease in the photodegradation of MB with increasing initial MB concentration. Fig. 5 shows a typical photocatalytic degradation process of MB (initial concentration: 20 mg/l, 50 ml) using 0.05 g Fe doped NiO nanoparticles under visible light irradiation. The absorption peaks corresponding to MB diminished gradually as the exposure time was extended.

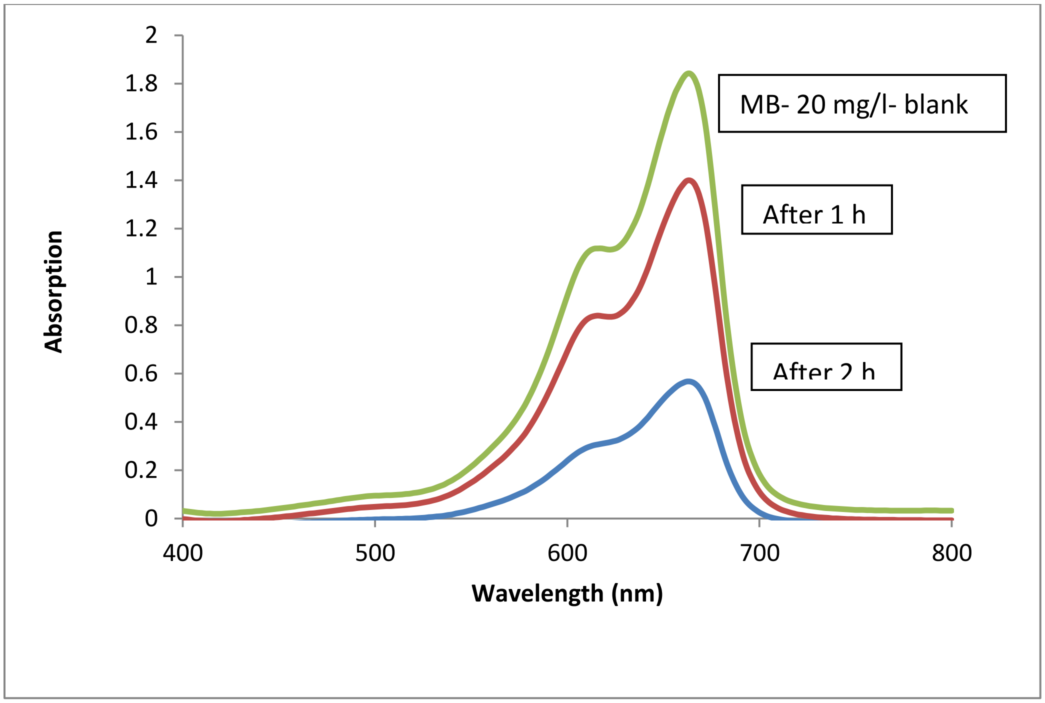

Fig. 5. The absorption spectra of the MB solution (initial concentration: 20 mg/l, 50 ml) in presence of Fe doped NiO nanoparticles (0.05 g) under visible light irradiation.

4. Conclusion

Fe doped NiO nanoparticles were synthesized by using a ball-mill mechanochemical technique at 2000 rpm at room temperature for 20 min. The photocatalytic degradation of MB in water was studied using prepared Fe doped NiO nanoparticles under visible light irradiation. The obtained results indicate that this semiconductor is a good photocatalyst under visible light.

References

[1] Hyo-Joong Kim, Kwon-Il Choi, Kang-Min Kim, Chan Woong Na, Jong-Heun Lee, Highly sensitive C2H5OH sensors using Fe-doped NiO hollow spheres, Sensors and Actuators B 171–172 (2012) 1029– 1037.

[2] N. Barsan, U. Weimar, Conduction model of metal oxide gas sensors, Journal of Electroceramics 7 (2001) 143–167.

[3] J.-H. Lee, Gas sensors using hierarchical and hollow oxide nanostructures, Sensors and Actuators B 140 (2009) 319–336.

[4] N. Yamazoe, New approaches for improving semiconductor gas sensors, Sensors and Actuators B 5 (1991) 7–19.

[5] N. Barsan, C. Simion, T. Heine, S. Pokhrel, U. Weimar, Modeling of sensing and transduction for p-type semiconducting metal oxide based gas sensors, Journal of Electroceramics 25 (2011) 11–19.

[6] C.N. Xu, J. Tamaki, N. Miura, N. Yamazoe, Grain size effects on gas sensitivity of porous SnO2-based elements, Sensors and Actuators B 3 (1991) 147–155.

[7] S. Pokhrel, C.E. Simion, V. Quemener, N. Barsan, U. Weimar, Investigations of conduction mechanism in Cr2O3 gas sensing thick films by ac impedance